This article has been accepted for publication in a future issue of this journal, but has not been fully edited. Content may change prior to final publication. Citation information: DOI 10.1109/JIOT.2017.2777917, IEEE Internet of Things Journal

Joint Synchronization and Localization in Wireless Sensor Networks Using Semidefinite Programming

Yanbin Zou, Huaping Liu, and Qun Wan

***Abstract*—A new joint synchronization and localization method for wireless sensor networks (WSNs) using two-way exchanged time-stamps is proposed in this paper. The goal is to jointly localize and synchronize the source node, assuming that the locations and clock parameters of the anchor nodes are known. We first form the measurement model and derive the Cramér-Rao lower bound (CRLB). An analysis of the advantages and disadvantages of a recent scheme on joint synchronization and localization motivates us to develop a maximum likelihood estimator (MLE) that effectively resolves the issues of this existing scheme. A novel semidefinite programming method is then proposed to transform the nonconvex MLE problem into a convex optimization problem. Extensive simulation results are obtained to compare the synchronization and localization performances of proposed scheme and a few state-of-the-art existing schemes.**

***Index Term*-Synchronization and localization, maximum likelihood (ML), semidefinite programming (SDP).**

I. Introduction

Clock synchronization is the premise for most of the applications of wireless sensor networks (WSNs) that have been used in tracking, monitoring, and control [1], and will likely be a core part of the future internet of things. For example, power management and transmission scheduling among the nodes require all nodes to have a common time reference [2]. There are many clock-synchronization schemes [3], but the classical two-way message-exchange-based schemes remain to be the most commonly used ones.

There are two types of nodes in a general WSN: anchor nodes with known locations and source nodes whose positions are to be estimated. It is common and reasonable to assume that the anchor nodes are synchronized and the source nodes need to be synchronized. When time-of-arrival (TOA) measurements are used to localize the source nodes, a small clock difference between the source node and anchor nodes could lead to significant localization errors [4]–[7]. Joint time synchronization and localization in WSNs was first studied in [8]. Before that, these two issues were investigated separately; synchronization was studied mainly from protocol design perspectives while localization was studied from signal processing perspectives. With such approaches, even a moderate synchronization error could lead to a significant localization performance loss [9]. Recent joint synchronization and localization schemes aim to improve the performances of previous schemes that separately address synchronization and localization [4], [10], [11]. However, there are remaining issues with these schemes. For example, the scheme proposed in [10] requires three-way message exchanges to reach the Cramér-Rao lower bound (CRLB); the approaches that use averaging proposed in [4], [11], although simplify the problem formulation, have compromised performance bounds.

In this paper we propose a novel joint time-synchronization and localization algorithm that uses two-way exchanged time-stamps in WSNs to achieve an improved performance over recent schemes such as the one in [4]. Although the averaging strategy presented in [4] simplifies the original problem formulation, it deteriorates the performance bound because the simplified problem using averaging is different from the original problem when there are more than one round of message exchange. The method being proposed in this paper starts from the original problem formulation and develops a maximum likelihood estimator (MLE), followed by a semidefinite programming (SDP) technique to relax the nonconvex MLE problem into a convex problem. This technique performs better than the SDP algorithm in [4] at the expanse of a slightly higher computational complexity.

The rest of this paper is organized as follows. The measurements model and CRLB are given in Sec. II. In Sec. III, the advantages and disadvantages of the scheme in [4] are analyzed. An SDP technique to relax the nonconvex MLE problem into a convex problem is established in Sec. IV. Sec. V provides numerical results to evaluate the estimation performance of the proposed estimator, followed by conclusions in Sec. VI.

Notations: $\mathbf{I}_m$ denotes the $m \times m$ identity matrix; $\mathbf{1}_m$ is a column vector consisting of m ones; $\odot$ denotes the Hadamard product; $\|\cdot\|$ is the l_2 norm; $\mathbf{A}(:,i)$ denotes the ith column of matrix $\mathbf{A}$; and for arbitrary symmetric matrices of equal size, $\mathbf{A} \succeq \mathbf{B}$ means that $\mathbf{A} - \mathbf{B}$ is positive semidefinite.

II. Problem Description

A. Measurement Model

In a WSN consisting of M anchor nodes and one source node, for v-dimentions localization ($v = 1, 2$ or 3), let $\mathbf{s}_m \in \mathbb{R}^v$ be the position of the mth anchor node, $\mathbf{u} \in \mathbb{R}^v$ be the unknown position of the source node, and $d_m = \|\mathbf{u} - \mathbf{s}_m\|$ be the distance from the mth anchor node to the source node.

In the two-way message exchange synchronization scheme, the source and anchor nodes exchange messages as illustrated in Fig. 1. The relationship between the source node's local clock time and the reference time is

$$t_{\text{local},x} = \omega_x t + \theta_x \quad (1)$$

Y. Zou and Q. Wan are with the School of Electronic Engineering, University of Electronic Science and Technology of China, Chengdu, 611731, China (Email: 201311020327@std.uestc.edu.cn, wanqun@uestc.edu.cn).

Y. Zou and H. Liu are with the School of Electrical Engineering and Computer Science at the Oregon State University, Corvallis, OR 97331, U.S.A. (e-mail: zouya@oregonstate.edu, hliu@eecs.oregonstate.edu).

This article has been accepted for publication in a future issue of this journal, but has not been fully edited. Content may change prior to final publication. Citation information: DOI 10.1109/JIOT.2017.2777917, IEEE Internet of Things Journal

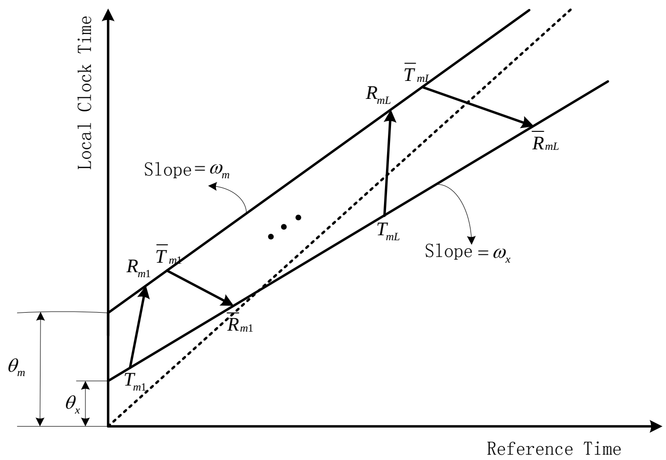

Fig. 1. Two-way message exchange between the source and the mth anchor nodes.

where $t_{\text{local},x}$ and t are the local time of the source node and the reference time, respectively, and ω_x and θ_x are the unknown clock skew and clock offset, respectively.

Similar, the relationship between the mth anchor node's local clock time and the reference time is

$$t_{\text{local},m} = \omega_m t + \theta_m \tag{2}$$

where $t_{\text{local},m}$ is the local time of the mth anchor node, and ω_m and θ_m are the known time skew and time offset, respectively.

Assume L rounds of message exchanges, and take the lth round for example: the source node transmits a signal at time T_{ml} and the mth anchor node receives it at time R_{ml}, which, at $\bar{T}_{ml}$, replies with a signal that contains the information of R_{ml} and $\bar{T}_{ml}$. The source node receives the reply signal at $\bar{R}_{ml}$. Note that T_{ml} and $\bar{R}_{ml}$ are the local time of the source node, and R_{ml} and $\bar{T}_{ml}$ are the local time of the mth anchor node. In a line-of-sight (LOS) propagation environment, the measured time stamps are expressed as [4], [12] (ch. 21), [13] (ch. 2)

$$R_{ml} = \frac{\omega_m}{\omega_x} T_{ml} + \omega_m(t_m + n_{ml}) - \frac{\omega_m}{\omega_x}\theta_x + \theta_m \tag{3a}$$

$$\bar{R}_{ml} = \frac{\omega_x}{\omega_m} \bar{T}_{ml} + \omega_x(t_m + \bar{n}_{ml}) - \frac{\omega_x}{\omega_m}\theta_m + \theta_x \tag{3b}$$

where $t_m = d_m/c$, c is the speed of light, n_{ml} and $\bar{n}_{ml}$ denote the measurement noises, which are modeled as i.i.d. zero-mean Gaussian variables with variance σ^2_{ml} and $\bar{\sigma}^2_{ml}$, respectively. It is reasonable to assume $\sigma^2_{ml} = \bar{\sigma}^2_{ml} = \sigma^2,\ m = 1, \cdots, M, l = 1, \cdots, L$.

B. CRLB for Joint Synchronization and Localization

Given the measurement model in (3), the performance of any unbiased estimator of $\boldsymbol{\kappa} = [\mathbf{u}^T, \omega_x, \theta_x]^T$ would be bounded by the CRLB. The CRLB of an estimator of $\boldsymbol{\kappa}$ is derived as follows.

From (3):

$$\frac{R_{ml}}{\omega_m} = \frac{T_{ml}}{\omega_x} + t_m - \frac{\theta_x}{\omega_x} + \frac{\theta_m}{\omega_m} + n_{ml} \tag{4a}$$

$$\bar{R}_{ml} = \frac{\omega_x}{\omega_m}\bar{T}_{ml} + \omega_x t_m - \frac{\omega_x}{\omega_m}\theta_m + \theta_x + \omega_x \bar{n}_{ml}. \tag{4b}$$

The Fisher information matrix (FIM) is calculated as [14]

$$\mathbf{I}(\boldsymbol{\kappa}) = \sum_{l=1}^{L} \mathbf{I}_{1l}(\boldsymbol{\kappa}) + \mathbf{I}_{2l}(\boldsymbol{\kappa}) \tag{5}$$

where

$$\mathbf{I}_{1l}(\boldsymbol{\kappa}) = \mathbf{q}_{1l}\mathbf{Q}^{-1}\mathbf{q}_{1l}^T \tag{6a}$$

$$\mathbf{I}_{2l}(\boldsymbol{\kappa}) = \frac{1}{\omega_x^2}\mathbf{q}_{2l}\mathbf{Q}^{-1}\mathbf{q}_{2l}^T \tag{6b}$$

$$\mathbf{q}_{1l}(:, m) = \left[\frac{(\mathbf{u}-\mathbf{s}_m)^T}{\|\mathbf{u}-\mathbf{s}_m\|\, c}, \frac{-(T_{ml}-\theta_x)}{\omega_x^2}, \frac{-1}{\omega_x}\right]^T \tag{6c}$$

$$\mathbf{q}_{2l}(:, m) = \left[\frac{\omega_x(\mathbf{u}-\mathbf{s}_m)^T}{\|\mathbf{u}-\mathbf{s}_m\|\, c}, \frac{(\bar{T}_{ml}-\theta_m)}{\omega_m} + \frac{\|\mathbf{u}-\mathbf{s}_m\|}{c}, 1\right]^T \tag{6d}$$

$$\mathbf{Q} = \sigma^2 \mathbf{I}_M. \tag{6e}$$

The CRLB on the variance of the unknown parameter $\boldsymbol{\kappa}$ is computed as

$$\mathrm{Var}([\boldsymbol{\kappa}]_i) \geq [\mathbf{I}^{-1}(\boldsymbol{\kappa})]_{i,i},\ i = 1, \cdots, v+2. \tag{7}$$

III. Joint Synchronization and Localization Using Averaging

In the cooperative joint synchronization and localization algorithm in WSNs developed in [4], the following variables are defined:

$$T_m = \frac{1}{L}\sum_{l=1}^{L} T_{ml},\ R_m = \frac{1}{L}\sum_{l=1}^{L} R_{ml} \tag{8a}$$

$$\bar{T}_m = \frac{1}{L}\sum_{l=1}^{L} \bar{T}_{ml},\ \bar{R}_m = \frac{1}{L}\sum_{l=1}^{L} \bar{R}_{ml}. \tag{8b}$$

Taking the average of (3) results in

$$R_m = \frac{\omega_m}{\omega_x} T_m + \omega_m(t_m + n_m) - \frac{\omega_m}{\omega_x}\theta_x + \theta_m \tag{9a}$$

$$\bar{R}_m = \frac{\omega_x}{\omega_m} \bar{T}_m + \omega_x(t_m + \bar{n}_m) - \frac{\omega_x}{\omega_m}\theta_m + \theta_x \tag{9b}$$

where n_m and $\bar{n}_m$ are zero-mean Gaussian random variables with the same variance of σ^2/L.

The CRLB on the variances of $\boldsymbol{\kappa}$ in model (9) can be derived similarly to the previous case. The FIM is calculated as

$$\hat{\mathbf{I}}(\boldsymbol{\kappa}) = \hat{\mathbf{I}}_1(\boldsymbol{\kappa}) + \hat{\mathbf{I}}_2(\boldsymbol{\kappa}) \tag{10}$$

where

$$\hat{\mathbf{I}}_1(\boldsymbol{\kappa}) = \hat{\mathbf{q}}_1\hat{\mathbf{Q}}^{-1}\hat{\mathbf{q}}_1^T \tag{11a}$$

$$\hat{\mathbf{I}}_2(\boldsymbol{\kappa}) = \frac{1}{\omega_x^2}\hat{\mathbf{q}}_2\hat{\mathbf{Q}}^{-1}\hat{\mathbf{q}}_2^T \tag{11b}$$

$$\hat{\mathbf{q}}_1(:,m) = \left[\frac{(\mathbf{u}-\mathbf{s}_m)^T}{\|\mathbf{u}-\mathbf{s}_m\|\,c}, \frac{-(T_m-\theta_x)}{\omega_x^2}, \frac{-1}{\omega_x}\right]^T \tag{11c}$$

$$\hat{\mathbf{q}}_2(:,m) = \left[\frac{\omega_x(\mathbf{u}-\mathbf{s}_m)^T}{\|\mathbf{u}-\mathbf{s}_m\|\,c}, \frac{(\bar{T}_m-\theta_m)}{\omega_m} + \frac{\|\mathbf{u}-\mathbf{s}_m\|}{c}, 1\right]^T \tag{11d}$$

$$\hat{\mathbf{Q}} = \sigma^2\mathbf{I}_M/L. \tag{11e}$$

The CRLB on the variance of the unknown parameter $\boldsymbol{\kappa}$ is computed as

$$\mathrm{Var}([\boldsymbol{\kappa}]_i) \geq [\hat{\mathbf{I}}^{-1}(\boldsymbol{\kappa})]_{i,i},\ i = 1,\cdots,v+2. \tag{12}$$

Proposition 1: The CRLB on the variance of $\boldsymbol{\kappa}$ with the model described by (9) is not smaller than that with the model given in (3).

Proof. For $L = 1$, it is easy to verify that the CRLB with the models given in (9) and (3) is the same.

For $L > 1$, we show that the CRLB based on model (9) is not smaller than that based on model (3). Note that the expressions $\mathbf{q}_{1l}(:,m)$ and $\hat{\mathbf{q}}_1(:,m)$ differ only in the $v+1$th element, and so are $\mathbf{q}_{2l}(:,m)$ and $\hat{\mathbf{q}}_2(:,m)$. Additionally, the averaging operator in (8) is linear; thus the elements of $\left(\mathbf{I}(\boldsymbol{\kappa}) - \hat{\mathbf{I}}(\boldsymbol{\kappa})\right)$ are zeros except the $v+1$th diagonal element, which is written as

$$\sum_{l=1}^{L}\sum_{m=1}^{M}\left[\frac{(T_{ml}-\theta_x)^2}{w_x^4} + (\frac{\bar{T}_{ml}-\theta_m}{w_m} + \frac{\|\mathbf{u}-\mathbf{s}_m\|}{c})^2\right] - L\sum_{m=1}^{M}\left[\frac{(T_m-\theta_x)^2}{w_x^4} + (\frac{\bar{T}_m-\theta_m}{w_m} + \frac{\|\mathbf{u}-\mathbf{s}_m\|}{c})^2\right]. \tag{13}$$

Eq. (13) is equivalent to

$$\sum_{l=1}^{L}\sum_{m=1}^{M}\left(\frac{T_{ml}^2}{w_x^4} + \frac{\bar{T}_{ml}^2}{w_m^2}\right) - L\sum_{m=1}^{M}\left(\frac{T_m^2}{w_x^4} + \frac{\bar{T}_m^2}{w_m^2}\right), \tag{14}$$

which can be split into the following two parts:

$$\sum_{l=1}^{L}\sum_{m=1}^{M}\frac{T_{ml}^2}{w_x^4} - L\sum_{m=1}^{M}\frac{T_m^2}{w_x^4}, \tag{15a}$$

$$\sum_{l=1}^{L}\sum_{m=1}^{M}\frac{\bar{T}_{ml}^2}{w_m^2} - L\sum_{m=1}^{M}\frac{\bar{T}_m^2}{w_m^2}. \tag{15b}$$

The time parameters T_{ml}, T_m, w_x, $\bar{T}_{ml}$, $\bar{T}_m$, as well as w_m are all positive. Applying Cauchy-Schwartz inequality yields

$$\sum_{l=1}^{L}T_{ml}^2 > L\left(\frac{1}{L}\sum_{l=1}^{L}T_{ml}\right)^2 = LT_m^2 \tag{16}$$

and

$$\sum_{l=1}^{L}\bar{T}_{ml}^2 > L\left(\frac{1}{L}\sum_{l=1}^{L}\bar{T}_{ml}\right)^2 = L\bar{T}_m^2. \tag{17}$$

The analysis above shows that

$$\mathbf{I}(\boldsymbol{\kappa}) - \hat{\mathbf{I}}(\boldsymbol{\kappa}) \succeq \mathbf{0}. \tag{18}$$

Therefore,

$$\mathbf{I}^{-1}(\boldsymbol{\kappa}) \preceq \hat{\mathbf{I}}^{-1}(\boldsymbol{\kappa}). \tag{19}$$

□

Proposition 1 shows that while the averaging strategy in [4] simplifies the original problem formulation, it also increases the CRLB of original problem.

IV. Proposed Algorithm

A. Maximum Likelihood Estimator

Here we formulate the maximum likelihood estimator (MLE), and in Sec. IV-B, we propose an SDP algorithm to solve this MLE problem. The time-stamp measurements n_{ml}, $\bar{n}_{ml}$, R_{ml}, T_{ml}, $\bar{R}_{ml}$, and $\bar{T}_{ml}$ are transformed into range measurements through $n_{ml}c$, $\bar{n}_{ml}c$, $R_{ml}c$, $T_{ml}c$, $\bar{R}_{ml}c$, and $\bar{T}_{ml}c$, respectively. From (3):

$$R_{ml}\beta_m = d_m + T_{ml}\beta_x - \alpha_x + \alpha_m + n_{ml} \tag{20a}$$

$$\bar{R}_{ml}\beta_x = d_m + \bar{T}_{ml}\beta_m + \alpha_x - \alpha_m + \bar{n}_{ml}. \tag{20b}$$

where $\beta_m = 1/\omega_m$, $\alpha_m = c\theta_m/\omega_m$, $\beta_x = 1/w_x$, and $\alpha_x = c\theta_x/\omega_x$. Let $\mathbf{h} = [\mathbf{u}^T, \beta_x, \alpha_x]^T$ represent the vector of the unknown parameters. The MLE problem is expressed as

$$\min_{\mathbf{h}} \sum_{l=1}^{L}\sum_{m=1}^{M}\frac{(R_{ml}\beta_m - d_m - T_{ml}\beta_x + \alpha_x - \alpha_m)^2}{\sigma^2} + \sum_{l=1}^{L}\sum_{m=1}^{M}\frac{(\bar{R}_{ml}\beta_x - d_m - \bar{T}_{ml}\beta_m - \alpha_x + \alpha_m)^2}{\sigma^2}. \tag{21}$$

B. Proposed Algorithm

An SDP algorithm is developed in this section to solve the MLE problem expressed in (21). The proposed algorithm is developed directly from model (3), which will perform better than the algorithm in [4], as shown by *Proposition 1*.

The MLE problem in (21) is written in a compact form as

$$\min_{\mathbf{u},\mathbf{y}} \sum_{l=1}^{L}\left\|\mathbf{R}_l\odot\boldsymbol{\beta} - \mathbf{d} - \boldsymbol{\alpha} - \mathbf{A}_l\mathbf{y}\right\|^2 + \sum_{l=1}^{L}\left\|-\bar{\mathbf{T}}_l\odot\boldsymbol{\beta} - \mathbf{d} + \boldsymbol{\alpha} - \mathbf{H}_l\mathbf{y}\right\|^2 \tag{22}$$

where $\mathbf{R}_l = [R_{1l},\cdots,R_{Ml}]^T$, $\mathbf{T}_l = [T_{1l},\cdots,T_{Ml}]^T$, $\bar{\mathbf{R}}_l = [\bar{R}_{1l},\cdots,\bar{R}_{Ml}]^T$, $\bar{\mathbf{T}}_l = [\bar{T}_{1l},\cdots,\bar{T}_{Ml}]^T$, $\boldsymbol{\beta} = [\beta_1,\cdots,\beta_M]^T$, $\boldsymbol{\alpha} = [\alpha_1,\cdots,\alpha_M]^T$, $\mathbf{d} = [d_1,\cdots,d_M]^T$, $\mathbf{A}_l = [\mathbf{T}_l, -\mathbf{1}_M]$, $\mathbf{H}_l = [-\bar{\mathbf{R}}_l, \mathbf{1}_M]$, and $\mathbf{y} = [\beta_x, \alpha_x]^T$.

Instead of estimating $\mathbf{u}$ and $\mathbf{y}$ jointly, $\mathbf{y}$ can be expressed as a function of $\mathbf{u}$. Letting the gradient of the objective function in (22) with respect to $\mathbf{y}$ to zero as below

$$-2\sum_{l=1}^{L}\mathbf{A}_l^T(\mathbf{R}_l\odot\boldsymbol{\beta} - \boldsymbol{\alpha} - \mathbf{d} - \mathbf{A}_l\mathbf{y}) - 2\sum_{l=1}^{L}\mathbf{H}_l^T(-\bar{\mathbf{T}}_l\odot\boldsymbol{\beta} + \boldsymbol{\alpha} - \mathbf{d} - \mathbf{H}_l\mathbf{y}) = \mathbf{0}, \tag{23}$$

This article has been accepted for publication in a future issue of this journal, but has not been fully edited. Content may change prior to final publication. Citation information: DOI 10.1109/JIOT.2017.2777917, IEEE Internet of Things Journal

yields

$$\mathbf{y} = \mathbf{g} - \mathbf{G}\mathbf{d} \tag{24}$$

where

$$\mathbf{g} = \left[\sum_{l=1}^{L}(\mathbf{A}_l^T\mathbf{A}_l + \mathbf{H}_l^T\mathbf{H}_l)\right]^{-1} \cdot \sum_{l=1}^{L}\left[(\mathbf{A}_l^T(\mathbf{R}_l\odot\boldsymbol{\beta} - \boldsymbol{\alpha}) + \mathbf{H}_l^T(-\bar{\mathbf{T}}_l\odot\boldsymbol{\beta}+\boldsymbol{\alpha})\right] \tag{25a}$$

$$\mathbf{G} = \left[\sum_{l=1}^{L}(\mathbf{A}_l^T\mathbf{A}_l + \mathbf{H}_l^T\mathbf{H}_l)\right]^{-1}\sum_{l=1}^{L}(\mathbf{A}_l^T + \mathbf{H}_l^T). \tag{25b}$$

Substituting (24) into (22) results in the optimization problem expressed as

$$\min_{\mathbf{u},\mathbf{d}} \sum_{l=1}^{L}\|\mathbf{R}_l\odot\boldsymbol{\beta} - \boldsymbol{\alpha} - \mathbf{A}_l\mathbf{g} + (\mathbf{A}_l\mathbf{G} - \mathbf{I}_M)\mathbf{d}\|^2 + \sum_{l=1}^{L}\left\|-\bar{\mathbf{T}}_l\odot\boldsymbol{\beta}+\boldsymbol{\alpha}-\mathbf{H}_l\mathbf{g}+(\mathbf{H}_l\mathbf{G}-\mathbf{I}_M)\mathbf{d}\right\|^2 \tag{26a}$$

$$\text{s.t.} \quad d_m = \|\mathbf{u} - \mathbf{s}_m\|, m = 1, \cdots, M. \tag{26b}$$

Define

$$\mathbf{e}_l = \mathbf{R}_l\odot\boldsymbol{\beta} - \boldsymbol{\alpha} - \mathbf{A}_l\mathbf{g} \tag{27a}$$

$$\mathbf{f}_l = -\bar{\mathbf{T}}_l\odot\boldsymbol{\beta} + \boldsymbol{\alpha} - \mathbf{H}_l\mathbf{g} \tag{27b}$$

$$\mathbf{E}_l = \mathbf{A}_l\mathbf{G} - \mathbf{I}_M \tag{27c}$$

$$\mathbf{F}_l = \mathbf{H}_l\mathbf{G} - \mathbf{I}_M. \tag{27d}$$

The optimization problem in (26) can be written as

$$\min_{\mathbf{u},\mathbf{d}} \ \mathbf{d}^T\sum_{l=1}^{L}\left[(\mathbf{E}_l^T\mathbf{E}_l+\mathbf{F}_l^T\mathbf{F}_l)\ \mathbf{d}+2(\mathbf{E}_l^T\mathbf{e}_l+\mathbf{F}_l^T\mathbf{f}_l)\right] \tag{28a}$$

$$\text{s.t.} \quad d_m = \|\mathbf{u} - \mathbf{s}_m\|, m = 1, \cdots, M. \tag{28b}$$

where the constant terms are discarded since they do not affect the optimization results.

Finally, by using the semidefinite relaxation (SDR) [15] method, (28) is rewritten into an SDP problem as

$$\min_{\mathbf{u},y_s,\mathbf{d},\mathbf{D}} \ \text{tr}\left(\mathbf{D}\sum_{l=1}^{L}(\mathbf{E}_l^T\mathbf{E}_l+\mathbf{F}_l^T\mathbf{F}_l)\right)+2\mathbf{d}^T\sum_{l=1}^{L}(\mathbf{E}_l^T\mathbf{e}_l+\mathbf{F}_l^T\mathbf{f}_l) \tag{29a}$$

$$\text{s.t.} \quad \mathbf{D}_{m,m} = \mathbf{y}_s - 2\mathbf{u}^T\mathbf{s}_m + \mathbf{s}_m^T\mathbf{s}_m, \ m = 1, \cdots, M \tag{29b}$$

$$\mathbf{D}_{i,j} \geq |\mathbf{y}_s - \mathbf{u}^T(\mathbf{s}_i+\mathbf{s}_j)+\mathbf{s}_i^T\mathbf{s}_j|, \ 1 \leq i < j \leq M. \tag{29c}$$

$$\begin{bmatrix} 1 & \mathbf{d}^T \\ \mathbf{d} & \mathbf{D}\end{bmatrix} \succeq \mathbf{0} \tag{29d}$$

$$\begin{bmatrix} \mathbf{I}_2 & \mathbf{u} \\ \mathbf{u}^T & \mathbf{y_s}\end{bmatrix} \succeq \mathbf{0} \tag{29e}$$

where (29c) is obtained by using the Cauchy-Schwartz inequality.

Next, we use the estimated $\hat{\mathbf{u}}$ to calculate $d_m = \|\hat{\mathbf{u}} - \mathbf{s}_m\|$, and then substitute it into (24) to estimate $\mathbf{y}$. Once $\mathbf{y}$ is determined, the estimates of clock skew and clock offset are expressed as

$$\hat{\omega}_x = 1/y(1) \tag{30a}$$

$$\hat{\theta}_x = y(2)/(cy(1)). \tag{30b}$$

Simulation results as will be shown in the next section reveal an interesting phenomenon: when $L = 1$, the smallest eigenvalue of matrix $\sum_{l=1}^{L}(\mathbf{E}_l^T\mathbf{E}_l + \mathbf{F}_l^T\mathbf{F}_l)$ is very close to zero. Thus the proposed algorithm (29) cannot effectively provide a solution. Similar to the approach adopted in [16], we also introduce the second-order-cone constraints and a penalty term to improve the accuracy of (29) for $L = 1$. This results in the following algorithm:

$$\min_{\mathbf{u},y_s,\mathbf{d},\mathbf{D}} \ \text{tr}(\mathbf{D}\sum_{l=1}^{L}(\mathbf{E}_l^T\mathbf{E}_l + \mathbf{F}_l^T\mathbf{F}_l))+ 2\mathbf{d}^T\sum_{l=1}^{L}(\mathbf{E}_l^T\mathbf{e}_l + \mathbf{F}_l^T\mathbf{f}_l) + \eta\text{tr}(\mathbf{D}) \tag{31a}$$

$$\text{s.t.} \quad \mathbf{D}_{m,m} = \mathbf{y}_s - 2\mathbf{u}^T\mathbf{s}_m + \mathbf{s}_m^T\mathbf{s}_m, \ i = m, \cdots, M. \tag{31b}$$

$$\|\mathbf{u} - \mathbf{s}_m\| \leq d_m, \ m = 1, \cdots, M. \tag{31c}$$

$$\mathbf{D}_{i,j} \geq |\mathbf{y}_s - \mathbf{u}^T(\mathbf{s}_i + \mathbf{s}_j) + \mathbf{s}_i^T\mathbf{s}_j|, \ 1 \leq i < j \leq M. \tag{31d}$$

$$\begin{bmatrix} 1 & \mathbf{d}^T \\ \mathbf{d} & \mathbf{D}\end{bmatrix} \succeq \mathbf{0} \tag{31e}$$

$$\begin{bmatrix} \mathbf{I}_2 & \mathbf{u} \\ \mathbf{u}^T & \mathbf{y_s}\end{bmatrix} \succeq \mathbf{0} \tag{31f}$$

where η is a regularization factor. Similar to [16], we also take K constant values $\eta_k, \ k = 1, \cdots, K$ to compute (31), and then use the estimated results $\hat{\mathbf{u}}_k, \ k = 1, \cdots, K$ to select the optimal $\hat{\mathbf{u}}$ that results in the minimum cost function J_k expressed as

$$J_k = \mathbf{d}_k^T\left[\sum_{l=1}^{L}(\mathbf{E}_l^T\mathbf{E}_l+\mathbf{F}_l^T\mathbf{F}_l)\mathbf{d}_k+2(\mathbf{E}_l^T\mathbf{e}_l+\mathbf{F}_l^T\mathbf{f}_l)\right] \quad k = 1, \cdots, K. \tag{32}$$

where $\hat{\mathbf{d}}_k = [\hat{d}_{k1}, \cdots, \hat{d}_{kM}]^T$ and $\hat{d}_{km} = \|\hat{\mathbf{u}}_k - \mathbf{s}_m\|, \ m = 1, \cdots, M$.

V. Simulation Results and Discussions

The performances of the proposed SDP algorithms (labeled as: 'Proposed A' and 'Proposed B', correspond to (29) and (31), respectively), a recent SDP algorithm proposed in [4], and SEP [9] (a two-step approach: synchronization using the scheme in [2] and then localization using the synchronization results [17]) are simulated and compared. The two proposed algorithms and the scheme developed in [4] are implemented in CVX toolbox [18] using SeDuMi as a solver [19]. In the following figures, the CRLB on the variance of $\boldsymbol{\kappa}$ with model (3) is labeled CRLB; the CRLB on the variance of $\boldsymbol{\kappa}$ with model (9) is labeled ACRLB.

This article has been accepted for publication in a future issue of this journal, but has not been fully edited. Content may change prior to final publication. Citation information: DOI 10.1109/JIOT.2017.2777917, IEEE Internet of Things Journal

The performance metric chosen is the root mean-square errors (RMSEs), which include location, clock skew, and clock offset, and are, respectively, defined as

$$\mathrm{RMSE_{lo}} = \sqrt{\tfrac{1}{N}\sum_{j=1}^{N}\|\hat{\mathbf{u}}_j - \mathbf{u}\|^2}$$
$$\mathrm{RMSE_{cs}} = \sqrt{\tfrac{1}{N}\sum_{j=1}^{N}(\hat{\omega}_{xj} - \omega_x)^2}$$
$$\mathrm{RMSE_{co}} = \sqrt{\tfrac{1}{N}\sum_{j=1}^{N}(\hat{\theta}_{xj} - \theta_x)^2}$$

where N is the number of Monte Carlo runs, $\hat{\mathbf{u}}_j$, $\hat{\omega}_{xj}$, and $\hat{\theta}_{xj}$ are, respectively, the estimates of the source node position, the source node clock skew, and the source node clock offset in the jth run. A total of $N = 1000$ Monte Carlo realizations are generated for each of the cases.

A WSN with four anchor nodes and one source node in 2-D plane is considered. Here, in order to avoid flip ambiguity [20]–[22], the positions of the anchor nodes, chosen so that they are not collinear, are $[20, 20]^T m$, $[20, -20]^T m$, $[-20, 20]^T m$, $[-20, -20]^T m$. The location of the source node is randomly generated in a square: $[-30, 30]m \times [-30, 30]m$. The clock offset and skew of the nodes are drawn from uniform distributions $U[1, 10]ns$ and $U[0.998, 1.002]$, respectively. The transmission times of the nodes T_{ml} and $\bar{T}_{ml}$ are drawn from uniform distributions $U[5l, 5l + 1] \times 10^{-5}s$ and $U[5l+3, 5l+4]\times 10^{-5}s$, respectively. The range measurement noise is a zero-mean Gaussian variable with variance σ^2.

Figs. 2-4 show the performances of the algorithms versus σ assuming $L = 4$. The CRLB on the variance of $\boldsymbol{\kappa}$ with model (9) is clearly higher than that with model (3), and the RMSEs with algorithm [4] is larger than the ACRLB. Additionally, Fig. 2 shows that the location estimate accuracy of ‘Proposed A’ is superior to the that of SEP and is lower than the ACRLB. The estimated results of clock skew and clock offset are shown in Fig. 3 and Fig. 4, respectively. It is observed that both ‘Proposed A’ and SEP could approach the CRLB. The results of ‘Proposed B’ are not included in these figures, because for $L > 1$, ‘Proposed B’ has the same performance as ‘Proposed A‘ when $L > 1$.

Figs. 5-7 show the performances of the algorithms versus σ assuming $L = 2$. A comparison between $L = 4$ and $L = 2$ reveals the following observation: the more rounds of message exchanges the better performance.

Figs. 8-10 evaluate the performances of the various algorithms versus σ assuming $L = 1$. In the computation for algorithm ‘Proposed B’, η is set to $10^{-4}, 10^{-3}, 10^{-2}, 10^{-1}, 10^{0}$. From the three figures, it is observed that the CRLBs on the variance of $\boldsymbol{\kappa}$ with model (9) and model (3) are identical, as we had discussed earlier in the paper. In that case, SEP is found to perform the worst. The reason is that SEP is a two-step algorithm, in which when $L = 1$ the first step (synchronization) has a poor performance, which directly degrades the performance of localization (in the second step) that uses the time skew and offset estimates of the first step. When $L = 1$, the performance of the first step is poor because the matrix that needs to be inverted in the least squares based algorithm has a large condition number. ‘Proposed B’ performs the best. Fig. 8 shows that the location estimation accuracy with algorithm [4] is slightly better than that with ‘Proposed A’. However, Figs. 9-10 show that the clock skew and clock offset estimate accuracies of algorithm [4] are worse than that with ‘Proposed A’.

TABLE I
THE AVERAGE RUNNING TIME [S] OF THE CONSIDERED ALGORITHMS. CPU: INTEL CORE 3 2.4 GHZ

Algorithms.	$L = 4$	$L = 2$	$L = 1$
Proposed A	0.5278	0.5197	0.5146
Algorithm in [4]	0.3401	0.3399	0.3414
Algorithm SEP	0.0025	0.0025	0.0025

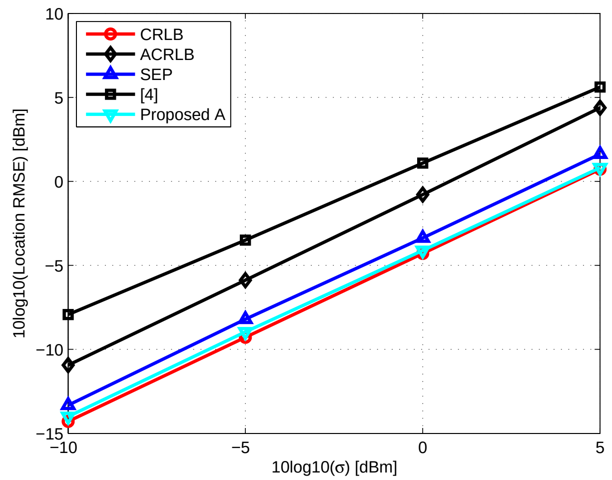

Fig. 2. RMSE of location estimate vs. σ $(L = 4)$.

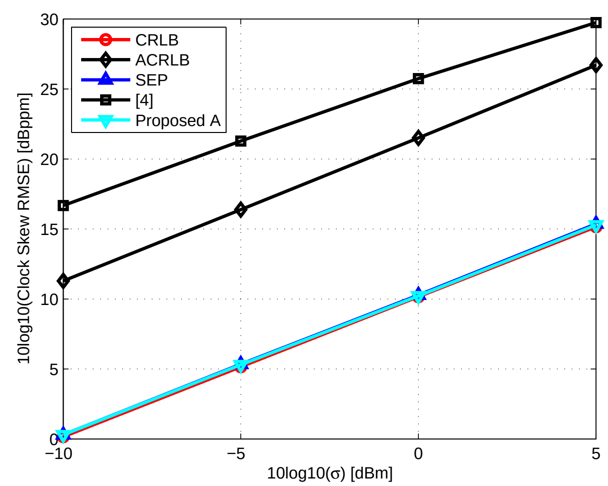

Fig. 3. RMSE of clock skew estimate vs. σ $(L = 4)$.

The SEP algorithm is based on the least squares method; therefore, its computational complexity is lower than that of the SDP based algorithms, i.e., the proposed algorithm and the algorithm [4]. Here we list the relative running time of ‘Proposed A’, the algorithm [4], and the SEP algorithm obtained in experiments in Table I. It is observed that ‘Proposed A’ requires a slightly more running time than the SDP

This article has been accepted for publication in a future issue of this journal, but has not been fully edited. Content may change prior to final publication. Citation information: DOI 10.1109/JIOT.2017.2777917, IEEE Internet of Things Journal

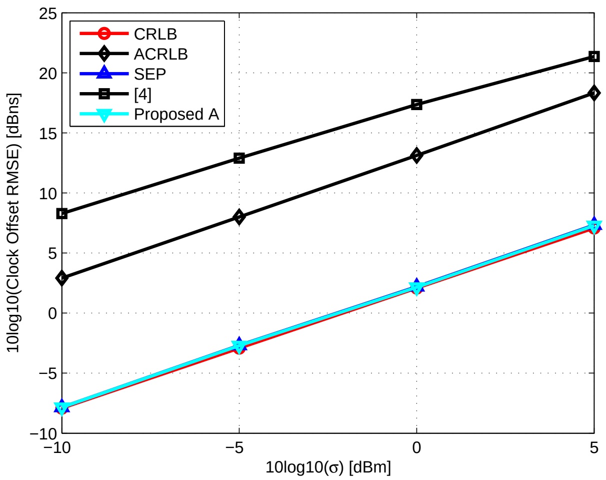

Fig. 4. RMSE of clock offset estimate vs. σ $(L = 4)$.

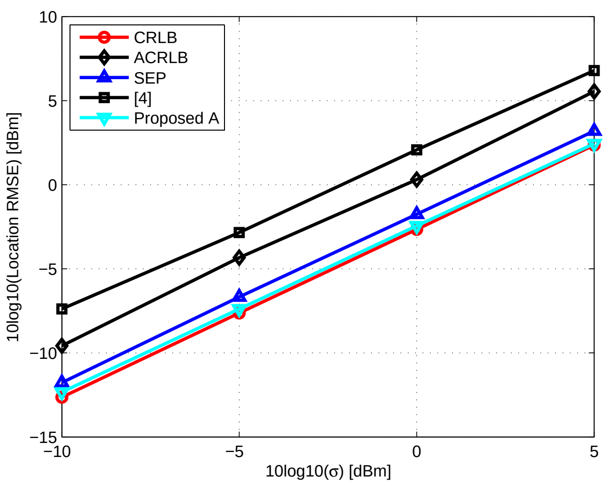

Fig. 5. RMSE of location estimate vs. σ $(L = 2)$.

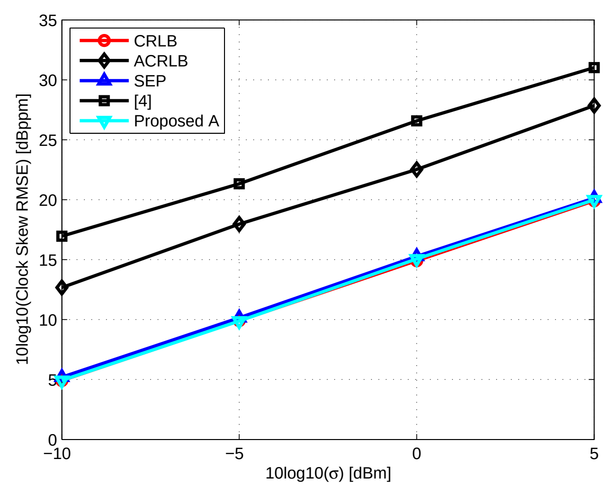

Fig. 6. RMSE of clock skew estimate vs. σ $(L = 2)$.

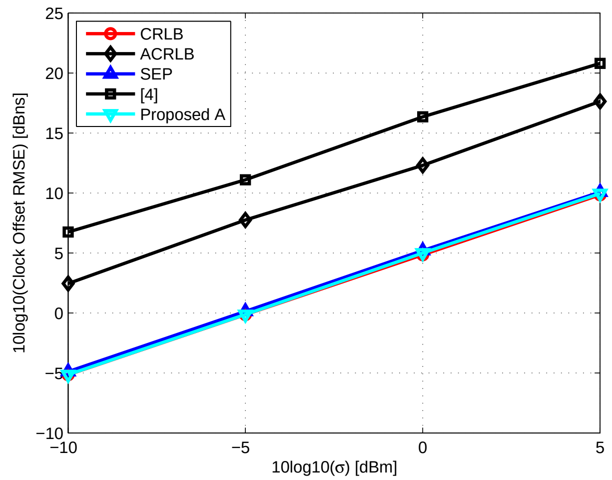

Fig. 7. RMSE of clock offset estimate vs. σ $(L = 2)$.

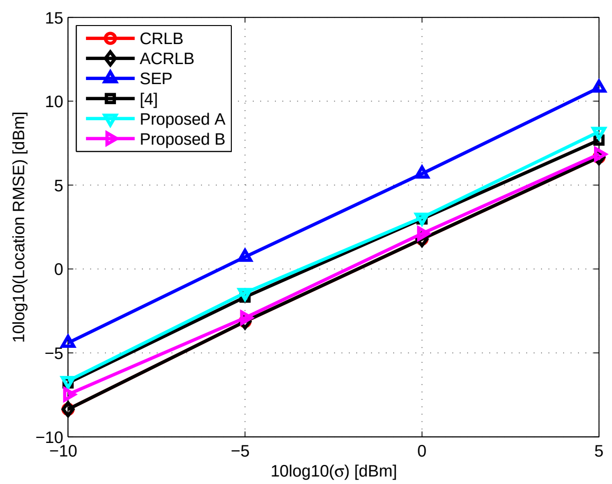

Fig. 8. RMSE of location estimate vs. σ $(L = 1)$.

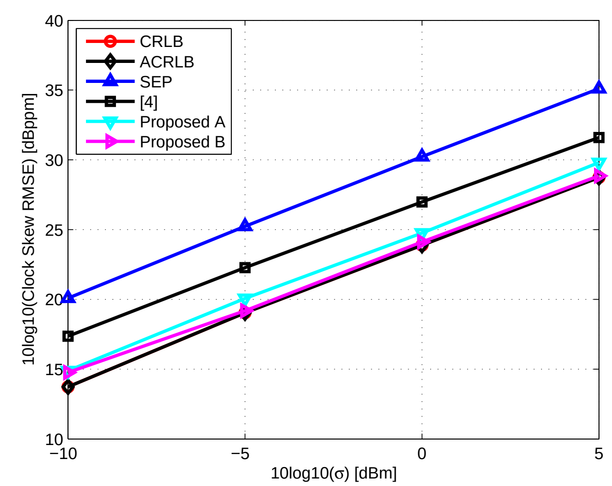

Fig. 9. RMSE of clock skew estimate vs. σ $(L = 1)$.

This article has been accepted for publication in a future issue of this journal, but has not been fully edited. Content may change prior to final publication. Citation information: DOI 10.1109/JIOT.2017.2777917, IEEE Internet of Things Journal

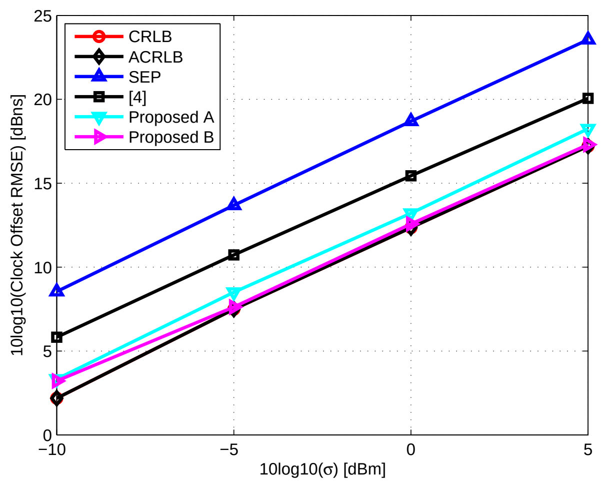

Fig. 10. RMSE of clock offset estimate vs. σ $(L = 1)$.

algorithm in [4], because 'Proposed A' has more constraints, i.e., (29c). The SEP algorithm requires the least amount of time as expected.

For large networks where there are many source nodes, requiring more than one round of message exchange is strongly discouraged, because each two-way message exchange would require some sort of resources for multiple access, for example, time or frequency or spatial resources, which are limited. Besides, the the source nodes are quite often power limited to require as fewer rounds of message exchanges are possible. Thus $L = 1$ is an important deployment scenario for systems with many source nodes. For this important deployment scenario, the proposed algorithm is superior to the SEP algorithm and the algorithm in [4] in terms of accuracy, albeit at the expense of a higher computational complexity. As computing power increases and parallel processing becomes more widely used, for performance-sensitive applications, the proposed scheme is attractive.

VI. Conclusions

The problem of joint synchronization and localization in WSNs by using two-way-exchanged time-stamp measurements is investigated. An analysis of an existing algorithm reveals that the averaging strategy may simplify the original problem formulation, but it deteriorates the performance bound. We thus propose a new SDP algorithm for joint synchronization and localization of the original problem. Numerical results of the proposed algorithms and some existing (recent) algorithms are obtained for performance comparison. For most cases, the MSE performance of location, clock skew, and clock offset estimates with the proposed schemes are superior to that with existing schemes, albeit at the expenses of an increased algorithm running time.

VII. Acknowledgment

The authors would like to thank the thorough reviews by the anonymous reviewers that have significantly helped us improve the presentation in this paper. This work was supported in part by the National Natural Science Foundation of China (NSFC) under Grant U1533125, 61471153 and 61771108, National Science and technology major project under Grant 2016ZX03001022, the Fundamental Research Funds for the Central Universities under Grant ZYGX2015Z011, and China Scholarship Council.

References

[1] A. H. Sayed, A. Tarighat, and N. Khajehnouri, "Network-based wireless location: challenges faced in developing techniques for accurate wireless location information," *IEEE Signal Process. Mag.*, vol. 22, no. 4, pp. 24–40, July 2005.

[2] M. Leng and Y.-C. Wu, "On clock synchronization algorithms for wireless sensor networks under unknown delay," *IEEE Trans. Veh. Technol.*, vol. 59, no. 1, pp. 182–190, Jan. 2010.

[3] Y. C. Wu, Q. Chaudhari, and E. Serpedin, "Clock synchronization of wireless sensor networks," *IEEE Signal Process. Mag.*, vol. 28, no. 1, pp. 124–138, Jan. 2011.

[4] R. M. Vaghefi and R. M. Buehrer, "Cooperative joint synchronization and localization in wireless sensor networks." *IEEE Trans. Signal Processing*, vol. 63, no. 14, pp. 3615–3627, July 2015.

[5] P. Oğuz-Ekim, J. Gomes, P. Oliveira, M. R. Gholami, and E. G. Ström, "Tw-toa based cooperative sensor network localization with unknown turn-around time," in *Acoustics, Speech and Signal Processing (ICASSP), IEEE International Conference on*, 2013, pp. 6416–6420.

[6] M. R. Gholami, S. Gezici, and E. G. Ström, "Tw-toa based positioning in the presence of clock imperfections," *Digital Signal Processing*, vol. 59, pp. 19–30, Dec. 2016.

[7] S. Gao, S. Zhang, G. Wang, and Y. Li, "Robust second-order cone relaxation for tw-toa-based localization with clock imperfection," *IEEE Signal Processing Letters*, vol. 23, no. 8, pp. 1047–1051, Aug. 2016.

[8] J. Zheng and Y. C. Wu, "Joint time synchronization and localization of an unknown node in wireless sensor networks," *IEEE Trans. Signal Process.*, vol. 58, no. 3, pp. 1309–1320, Mar. 2010.

[9] R. M. Vaghefi and R. M. Buehrer, "Joint toa-based sensor synchronization and localization using semidefinite programming," in *IEEE International Conference on Communications (ICC)*, 2014, pp. 520–525.

[10] V. Y. Zhang and K. S. Wong, "Closed-form solution for joint localization and time synchronization in wireless sensor networks," in *IEEE International Conference on Communications (ICC)*, 2010, pp. 1–5.

[11] R. M. Vaghefi and R. M. Buehrer, "A linear estimator for joint synchronization and localization in wireless sensor networks," in *2014 IEEE Global Communications Conference*, 2014, pp. 505–510.

[12] R. Zurawski, *Industrial communication technology handbook*. CRC Press, 2014.

[13] M. Werner, *Indoor location-based services: Prerequisites and foundations*. Springer, 2014.

[14] S. M. Kay, "Fundamentals of statistical signal processing, volume i: estimation theory," 1993.

[15] S. Boyd and L. Vandenberghe, *Convex Optimization*. Cambridge, UK: Cambridge University Press, 2004.

[16] Y. Zou and Q. Wan, "Asynchronous time-of-arrival-based source localization with sensor position uncertainties," *IEEE Commun. Lett.*, vol. 20, no. 9, pp. 1860–1863, Sep. 2016.

[17] Y. T. Chan and K. Ho, "A simple and efficient estimator for hyperbolic location," *IEEE Trans. Signal Process.*, vol. 42, no. 8, pp. 1905–1915, Aug. 1994.

[18] M. Grant and S. Boyd, "Cvx: Matlab software for disciplined convex programming, version 1.21," http://cvxr.com/cvx, May 2010.

[19] J. F. Sturm, "Using sedumi 1.02, a matlab toolbox for optimization over symmetric cones," *Optimization Methods and Software*, vol. 11, no. 1-4, pp. 625–653, Mar. 1999.

[20] A. A. Kannan, B. Fidan, and G. Mao, "Analysis of flip ambiguities for robust sensor network localization," *IEEE transactions on vehicular technology*, vol. 59, no. 4, pp. 2057–2070, May 2010.

[21] W. Liu, E. Dong, and Y. Song, "Robustness analysis for node multilateration localization in wireless sensor networks," *Wireless Networks*, vol. 21, no. 5, pp. 1473–1483, July 2015.

[22] A. A. Kannan, G. Mao, and B. Vucetic, "Simulated annealing based wireless sensor network localization with flip ambiguity mitigation," in *IEEE 63rd Vehicular Technology Conference*, vol. 2, 2006-Spring, pp. 1022–1026.

This article has been accepted for publication in a future issue of this journal, but has not been fully edited. Content may change prior to final publication. Citation information: DOI 10.1109/JIOT.2017.2777917, IEEE Internet of Things Journal

Yanbin Zou (S'13) is currently working towards the Ph.D. degree in the Department of Electronic Engineering, University of Electronic Science and Technology of China (UESTC), Chengdu, China. His research interests include source localization and array signal processing.

Huaping Liu (S'95-M'97-SM'08) received the B.S. and M.S. degrees in electrical engineering from Nanjing University of Posts and Telecommunications, Nanjing, China, in 1987 and 1990, respectively, and the Ph.D. degree in electrical engineering from New Jersey Institute of Technology, Newark, in 1997. From July 1997 to August 2001, he was with Lucent Technologies, Whippany, New Jersey. In September 2001, he joined the School of Electrical Engineering and Computer Science, Oregon State University, Corvallis, Oregon, where he has been a full professor since 2011. His research interests include modulation and detection, multiple-antenna techniques, and localization systems.

Qun Wan (M'04) received the B.Sc. degree in electronic engineering from Nanjing University in 1993, the M.Sc. degree and Ph.D. degree from University of Electronic Science and Technology of China (UESTC) in 1996 and 2001 respectively, both in electronic engineering. From 2001 to 2003, he was a post-doctor with the Department of Electronic Engineering, Tsinghua University. Since 2004, he has been a professor with the Department of Electronic Engineering, UESTC. He is currently the Director of Joint Research Lab of Array Signal Processing and Associate Dean of School of Electronic Engineering. His research interests include direction finding, radio localization, and signal processing based on information criterion.